Stem cell therapy for cardiovascular disease : answering basic questions regarding cell behavior

Bogt, K.E.A. van der

CHAPTER 6

Comparison of Different Adult Stem Cell Types for Treatment of Myocardial Ischemia

Koen E.A. van der Bogt, Ahmad Y. Sheikh, Sonja Schrepfer, Grant Hoyt, Feng Cao, Katie Ransohoff, Rutger-Jan Swijnenburg, Jeremy Pearl, Michael Fischbein, Christopher H. Contag, Robert C. Robbins and Joseph C. Wu

Circulation 2008 Sep 30;118(14 Suppl):S121-9.

ABSTRACT

Introduction: A comparative analysis of the efficacy of different cell candidates for the treatment of heart disease remains to be described. This study is designed to evaluate the therapeutic efficacy of 4 cell types in a murine model of myocardial infarction.

Methods: Bone marrow mononuclear cells (MN), mesenchymal stem cells (MSC), skeletal myoblasts (SkMb) and fibroblasts (Fibro) were isolated from male L2G transgenic mice (FVB background) that constitutively express firefly luciferase (Fluc) and green fluorescence protein (GFP). Cells were characterized by flow cytometry, bioluminescence imaging (BLI), and luminometry. Female FVB mice (n=60) underwent LAD ligation and were randomized into 5 groups to intramyocardially receive one cell type (5×10^5) or PBS as control. Cell survival was measured *in vivo* by BLI and *ex vivo* by TaqMan PCR at week 6. Cardiac function was assessed by echocardiography and invasive hemodynamic measurements were made at week 6.

Results: Fluc expression correlated with the cell number in all groups ($r^2>0.93$). *In vivo* BLI revealed acute donor cell death of MSC, SkMb, and Fibro within 3 weeks after transplantation. By contrast, cardiac signals were still present after 6 weeks in the MN group, as confirmed by TaqMan PCR ($P<0.01$). Echocardiography showed significant preservation of fractional shortening in the MN group compared to controls ($P<0.05$). Measurements of left ventricular end-systolic/diastolic volumes revealed that the least amount of ventricular dilatation occurred in the MN group ($P<0.05$). Histology confirmed the presence of MN, although there was no evidence of transdifferentiation by donor MN into cardiomyocytes.

Conclusion: This is the first study to directly compare a variety of cell candidates for myocardial therapy. Compared to MSC, SkMB, and Fibro, our results suggest that MN cells exhibit a more favorable survival pattern, which translates into a more robust preservation of cardiac function.

INTRODUCTION

Coronary artery disease is the number one cause of morbidity and mortality in the US. Despite a wide range of therapeutic approaches, heart failure remains the leading cause of death in the Western world.[1] Recently, cell therapy has generated much enthusiasm as a novel potential treatment for ischemic heart disease. Numerous animal studies, each evaluating a particular class of cells for its regenerative potential in the infarcted heart, have been conducted.[2] Furthermore, the administration of skeletal myoblasts (SkMb)[3], bone marrow-derived mononuclear cells (MN)[4-6] and mesenchymal stem cells (MSC)[7] as a therapy for end-stage heart disease has already been translated from bench top to bedside. Although the majority of experimental studies have shown encouraging results, clinical outcomes are divergent, which highlights the present imperfect understanding of the *in vivo* behavior and the mechanism(s) of action of the cells.[8] Moreover, differences in cell type and dose, study design, patient population, and timing of cell transplant hamper inter-study comparisons.

Recently, molecular imaging has proven to be a valuable tool to track cells on an *in vivo* and quantitative bases in mice.[9] As opposed to post-mortem histology, molecular imaging is non-invasive and facilitates repetitive imaging, thereby providing unprecedented insight into cell position and count. These characteristics make molecular imaging an extremely useful method to monitor cell survival, proliferation, migration, and even misbehavior.[10] In order to understand which cell type will generate optimal therapeutic responses, we evaluated the efficacy of various therapeutic stem cell candidates in a uniform, controlled murine model of ischemic heart failure. Results gathered from this head-to-head comparison study should yield valuable information regarding the optimal cell type for cardiac regenerative therapy.

METHODS

Transgenic L2G animals expressing Fluc-GFP. All animal study protocols were approved by the Stanford Animal Research Committee. The donor group consisted of 8-week old male L2G mice (n=10), which were bred on FVB background and ubiquitously express green fluorescent protein (GFP) and firefly luciferase (Fluc) reporter genes driven by a β-actin promoter as previously described.[11] Recipient animals (n=70) consisted of syngeneic, female FVB mice (8 weeks old, Jackson Laboratories, Bar Harbor, ME, USA). To compare the efficacy of different adult stem cell types, animals were randomized into 5 recipient groups (n=12/group): (1) bone marrow derived mononuclear cells (MN), (2) skeletal myoblasts (SkMb), (3) bone marrow derived mesenchymal cells (MSC), (4) fibroblasts (Fibro), and (5) saline (PBS). To compare the effects of myocardial milieus on MN survival, animals were randomized into 2 recipient groups (n=5/group): (1) injection at the infarct site and (2) injection at the peri-infarct site.

Preparation of fibroblasts (Fibro). Donor mice were euthanized by cervical dislocation after anesthesia with 5% isoflurane, and were placed in 70% ethanol for 5 minutes. For the isolation of Fibro, skin biopsies were taken from the tail and ears, minced, and incubated overnight in collagenase type II (400 U/mL, Gibco-Invitrogen, Carlsbad, CA, USA,), dissolved in DMEM (Gibco, NY, USA) supplemented with 20% heat-inactivated fetal bovine serum (FBS, Hyclone, Logan, UT, USA), 1% antibiotics/antimycotic solution (penicillin/streptomycin, Gibco-Invitrogen, Carlsbad, CA, USA) at 37°C and 5% CO_2 in air.[12] The next day, cells were dislodged from digested tissue by repeated pipetting and were passed through 70 µm sterile netting into sterile 14-ml centrifuge tubes. The samples were centrifuged for 5 minutes at 1200 rpm, and the cell pellet was resuspended in DMEM, 20% FBS, 1% penicillin/streptomycin to be plated in a 25 cm^2 tissue flask at 37°C/5%CO_2.

Preparation of skeletal myoblasts (SkMb). After the skin was isolated, the muscles were dissected from the legs, minced, and placed in a Dispase solution (grade II, 2.4U/mL, Gibco-Invitrogen, Carlsbad, CA, USA) for 45 minutes under regular pipetting. The suspension was filtered through a 70 µm nylon mesh and was centrifuged at 1200 rpm for 5 minutes. The cell pellet was resuspended into 45% DMEM/45% Ham's F10 medium (Gibco-Invitrogen, Carlsbad, CA, USA), supplemented with 10% FBS and 1% penicillin/streptomycin and plated in 25 cm^2 collagen-coated tissue flasks. When confluent, cells were dislodged and passaged using PBS. Cells were grown for 5 passages, after which they were transferred into DMEM, 10% FBS, and 1% penicillin/streptomycin medium supplemented with 2.5 ng/mL Basic Fibroblast Growth Factor (Gibco-Invitrogen, Carlsbad, CA, USA) to achieve confluent SkMb cultures.[13]

Preparation of bone marrow mononuclear cells (MN) and mesenchymal stem cells (MSC). Finally, the long bones were explanted, washed, and flushed with PBS using a 25-gauge needle to collect bone marrow. After passing through a 70 µm strainer, the isolate was centrifuged at 1200 rpm for 5 minutes, washed, and resuspended into DMEM, 20% FBS, and 1% penicillin/streptomycin medium to grow MSC. All plated cells were allowed to grow for 6 passages before transplantation to avoid contamination with other cell types. To acquire the MN fraction, the bone marrow isolate was centrifuged for 40 minutes at 1600 rpm using a 14 mL tube with 3 mL Ficoll-Paque Premium (GE Healthcare, Piscataway, NJ, USA) gradient and 4 mL cell/saline suspension. MN were prepared freshly before application.

Characterization of stem cells by flow cytometry. Cells were incubated in 2% FBS/PBS at 4°C for 30 min with 1 µL monoclonal FITC-conjugated antibodies against CD34, CD45, C-kit, CD11b, and CD90 (BD, San Jose, CA, USA), and processed through a FACSCalibur system (BD, San Jose, CA, USA) according to the manufacturer's protocol.

***In vitro* firefly luciferase (Fluc) assays.** Cells were dislodged from culture flasks (SkMb, MSC and Fibro) or processed directly after isolation (MN) to be resuspended in PBS. Cell suspensions were divided into a 6-well plate in known concentrations. After administration of D-Luciferin (Xenogen, Alameda, CA, USA, 4.5ug/mL), peak signal expressed as photons per second per centimeter square per steridian (photons/s/cm^2/sr) was measured using a charged coupled device (CCD) camera (IVS200, Xenogen, Alameda, CA, USA) as described.[14] Same amounts of dislodged cells were lysed using 200 µL of 10X Passive Lysis Buffer (Promega, Madison, WI, USA) and centrifuged at maximum speed for 2 minutes at 4°C. For every sample, 20 µL supernatant was added to 100 µL Luciferase Assay Reagent (LAR-II, Promega, Madison, WI, USA) and luminosity in relative light units (RLU) was measured on a TD-20/20n luminometer (Turner Biosystems, Sunnyvale, CA, USA). All samples were conducted in triplets.

Surgical model for myocardial infarction. Female FVB mice (8 weeks old) were intubated with a 20-gauge angiocath (Ethicon Endo-Surgery, Inc. Cincinnati, OH) and placed under general anesthesia with isoflurane (2%). Myocardial infarction (MI) was created by ligation of the mid-left anterior descending (LAD) artery with 8-0 ethilon suture through a left anterolateral thoracotomy as described.[15] Ten minutes afterwards, the infarct region was confirmed by myocardial blanching. Injections were made at 2 sites near the peri-infarct zone (medial and lateral zones) with a total volume of 50 µL containing 5x10^5 cells or PBS respective of group randomization using a Hamilton syringe with a 29-gauge needle. All surgical procedures were performed in a blinded fashion by one micro-surgeon (G.H.) with several years of experience on this model.

***In vivo* optical bioluminescence imaging (BLI).** BLI was performed using the IVIS 200 (Xenogen, Alameda, CA, USA) system. Recipient mice were anesthetized with isoflurane, shaved, and placed in the imaging chamber. After acquisition of a baseline image, mice were intraperitoneally injected with D-Luciferin (400 mg/kg body weight). Mice were imaged on day 2, 4, 7, and weekly until sacrifice at week 6. Peak signals (photons/s/cm^2/sr) from a fixed region of interest (ROI) were evaluated as described.[11]

Echocardiography to assess left ventricular fractional shortening (LVFS). Echocardiography studies were performed 4 and 6 weeks post-operation. Three independent two-dimensional transversal-targeted M-mode traces were obtained at the level of the papillary muscles using a 14.7-MHz transducer on a Sequoia C512 Echocardiography system (Siemens, Malvern, PA, USA). Using the enclosed software, left ventricular end-diastolic and end-systolic posterior and anterior dimensions were measured by a blinded investigator (A.Y.S.) and processed to calculate left ventricular fractional shortening (LVFS).

Measurement of hemodynamics with pressure-volume loops. Invasive, steady-state hemodynamic measurements were conducted by closed-chest pressure-volume (PV) loop analysis prior to sacrifice at week 6. The animal was placed under general anesthesia as described above. After midline neck incision, a 1.4-F conductance catheter (Millar Instruments, Houston, TX, USA) was retrogradally advanced through the right carotid artery into the left ventricle. The measurements of segmental conductance were recorded which allowed extrapolation of the left ventricular volume, which was coupled with pressure. These data were analyzed in a blinded fashion using PVAN 3.4 Software (Millar Instruments, Houston, TX, USA) and Chart/Scope Software (AD Instruments, Colorado Springs, CO, USA).

***Ex vivo* TaqMan PCR.** In our protocol, the transplanted cells were derived from male mice and were transplanted into female recipients, which facilitate quantification of male cells in the explanted female hearts by tracking the Sry locus found on the Y chromosome. After the invasive hemodynamic measurements at week 6, animals were sacrificed and hearts were randomly selected for explantation, followed by mincing and homogenization in 2 mL DNAzol (Invitrogen, Carlsbad, CA, USA). DNA was isolated according to the manufacturer's protocol. The DNA was quantified on a ND-1000 spectrophotometer (NanoDrop Technologies, Wilmington, DE, USA) and 500 ng DNA was processed for TaqMan PCR using primers specific for the Sry locus. RT-PCR reactions were conducted in iCylcer IQ Real-Time Detection Systems (Bio-Rad, Hercules, CA, USA). Detection levels were compared to a standard curve to assess the number of viable cells per sample. All samples were conducted in triplets.

Postmortem histology. Hearts (n=3/group at week 2) were flushed with saline and placed in 2% paraformaldehyde for 2 hours at room temperature followed by 12-24 hours in 30% sucrose at 4°C. The tissue was embedded in Optical Cutting Temperature (OCT) Compound (Tissue-Tek. Sakura Finetek USA Inc., Torrance, CA) and snap frozen on dry ice. Five-micron sections were cut in both the proximal and apical regions of the infarct zone. Slides were stained for GFP (anti-green fluorescent protein, rabbit IgG fraction, anti-GFP Alexa Fluor 488 conjugate, 1:200, Molecular Probes, Inc.), troponin I (H-170 rabbit polyclonal IgG for cardiac muscle, 1:100, Santa Cruz Biotech, Santa Cruz, CA), and connexin 43 (rabbit polyclonal, 1:100, Sigma). Sections were counterstained with 4,6-diamidino-2-phenylindole (DAPI). Stained tissue was examined by Leica DMRB fluorescent microscope and a Zeiss LSM 510 two-photon confocal laser scanning microscope. Cell engraftment was confirmed by identification of GFP expression under fluorescent microscopy. Colocalization of troponin, alpha sarcomeric actin, and connexin 43 with GFP was visualized with streptavidin-conjugated to Alexa Fluor Red 555 (Invitrogen Molecular Probes, Carlsbad, CA).

Statistical analysis. Statistics were calculated using SPSS 14.0 (SPSS Inc., Chicago, IL, USA). Descriptive statistics included mean and standard error. Comparison between groups was performed using a one-way between groups ANOVA, or one-way repeated measures ANOVA when compared over time, and significance was assumed according to the Bonferroni-Holm's procedure.

Statement of Responsibility: The authors had full access to and take full responsibility for the integrity of the data. All authors have read and accept the manuscript as written.

Conflict of Interest Disclosures: None.

RESULTS

Cell characterization. The MN population consisted of $CD34^+$, $CD45^+$ and $CD11b^+$, representing portions of hematopoietic cells as well as macrophages, granulocytes, and natural killer cells (**figure 1a**).[16] After 6 passages of MSC, flow cytometry results showed absence of CD34, CD45 and C-kit markers (**figure 1b**), indicating depletion of hematopoeitic cells within the MSC. Moreover, these cells expressed the MSC markers CD90 and CD106, with negative expression of CD105 (data not shown). Myoblast cultures steadily differentiated into myotubes under high confluence or after prolonged culture without replating (**figure 2c-d**), which confirmed their fate.[13]

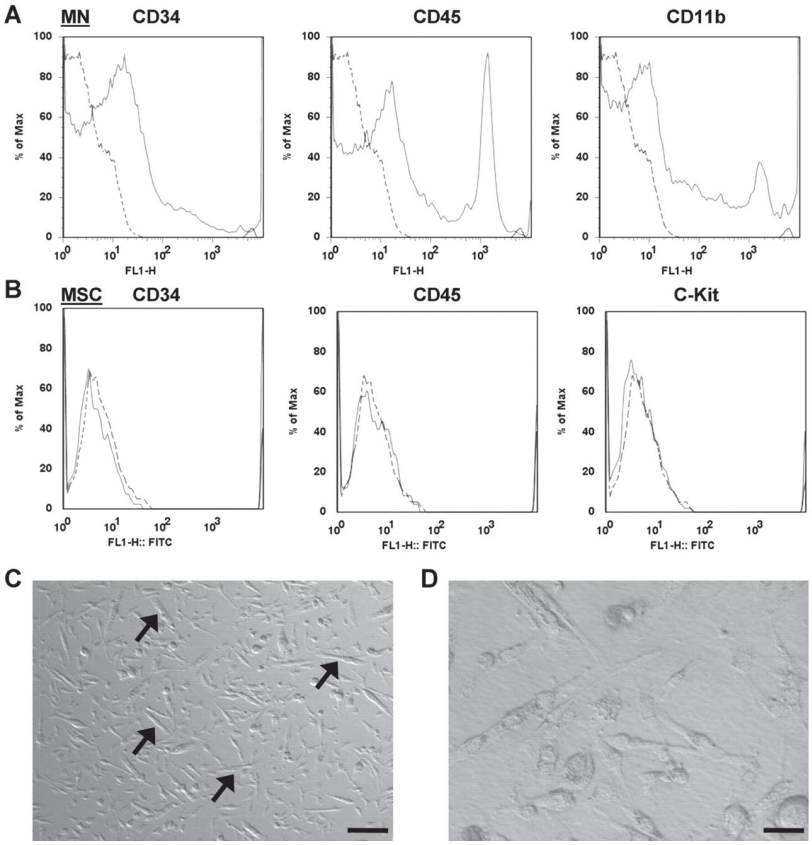

Figure 1. Characterization of cell types based on cell surface expression and cell morphology. (a) Flow cytometry results from bone marrow-derived mononuclear cells (MN) and (b) bone marrow-derived mesenchymal cells (MSC). Green lines represent isotype controls. (c) After prolonged non-passaged culture, skeletal myoblasts (SkMb) change morphologically (100x Bright-field Hoffman modulated contrast image, bar represents 40µm). (d) SkMb form longitudinal myotubes, confirming myoblast phenotype (400x Bright-field Hoffman modulated contrast image, bar represents 10 µm).

Firefly luciferase (Fluc) expression. After culturing for 6 passages, cells were processed for *ex vivo* BLI. Cell number correlated well with BLI signal in all groups (MN: r^2=0.98, SkMb: r^2=0.94, MSC: r^2=0.94, Fibro: r^2=0.93), indicating that BLI is a valid tool to assess cell viability. However, Fluc expression level differed per cell type, as MN showed poor *ex vivo* signal compared to other cell groups (**figure 2a-b**). We hypothesized this was a consequence of the Ficoll selection in the MN group, which may have accounted for hibernation of the cells due to the hostile environment, thereby preventing proper D-Luciferin uptake. In order to test this hypothesis, we lysed the cells and measured intracellular Fluc enzyme. Our *in vitro* luminometry results indeed showed that the Fluc enzyme was present in all cell types and correlated well with cell number (MN: r^2=0.99, SkMb: r^2=0.95, MSC: r^2=1.00, Fibro: r^2=0.93) (**figure 2c**). It also correlated well with the *ex vivo* BLI findings (MN: r^2=0.99, SkMb: r^2=0.98, MSC: r^2=0.90, Fibro: r^2=0.95; **figure 2d**). Thus, BLI is a reliable tool to measure viable cell numbers *ex vivo* and can be used instead of *in vitro* luminometry.

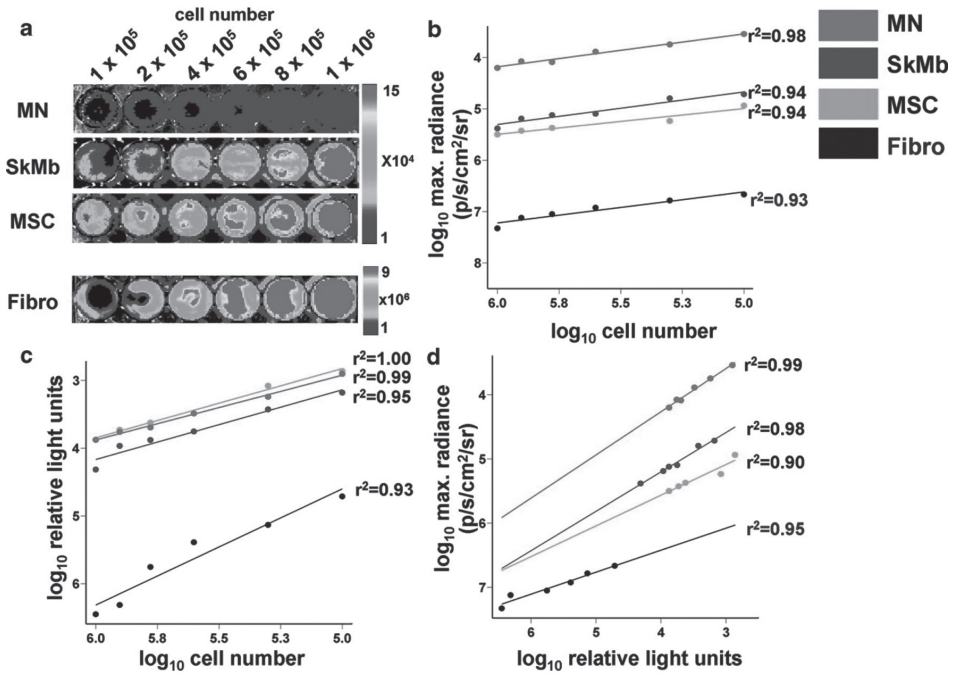

Figure 2. Optical bioluminescence imaging (BLI) signal from firefly luciferase (Fluc) expression reflects viable cell number. (a) BLI of varying numbers of cells in 24-well plates with increasing signals. Scale bars represent peak signal in photons/s/cm²/sr. Cell numbers from all cell types showed robust correlation with (b) Fluc signal on ex vivo BLI and (c) *in vitro* Fluc enzyme on luminometry. (d) Both assays (BLI and luminometry) also correlated well with each other.

***In vivo* kinetics and biodistribution of transplanted cells.** In our study, increasing BLI signals in the MN group suggested a growing number of cells from day 2 to week 2 post-transplant. Moreover, presence of extra-cardiac signals was consistent with migration to other organs such as the femur, spleen, and liver (**figure 3a**). In contrast, for SkMB, MSC, and Fibro, BLI signals decreased acutely from day 2 to week 2. By week 4, the BLI signals equaled background level (**figure 3b-e**). Interestingly, robust signals were seen at day 2 to day 4 in the lungs, suggesting leakage of SkMb, MSC, and Fibro with subsequent intracappillary retention. This might have accounted for the higher rates of acute-phase mortality in these groups (data not shown). In order to assess the effects of myocardial milieu on MN survival, we also compared infarct versus peri-infarct targeted injection. Similarly, we observed significant donor cell death after an initial increase in BLI signal and no major differences in the cell survival pattern between the two modes of injection after 4 weeks (**figure 4**).

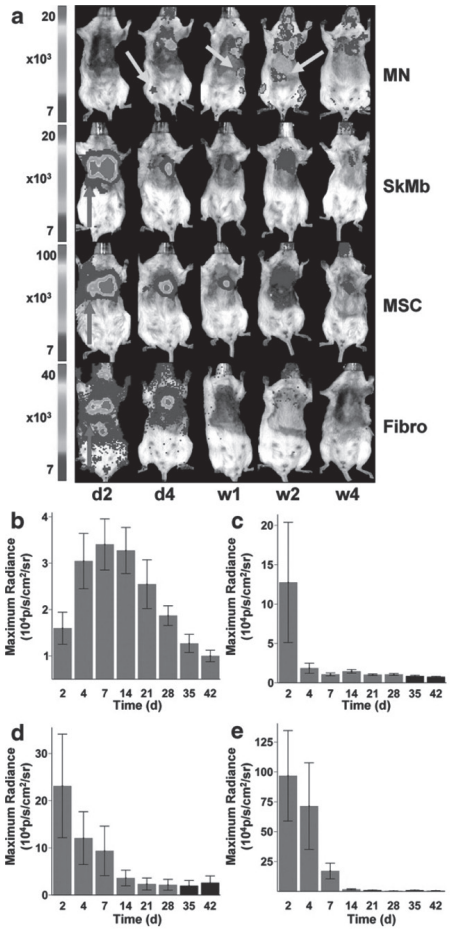

Figure 3. Longitudinal in vivo optical bioluminescence imaging (BLI) of transplanted cell survival. (a) Images from the same representative animal from each group reveal cell proliferation, death, and migration. MN show retention in the heart, and furthermore can home in on the femur, spleen, and liver (yellow arrows). BLI images from animals 2 days after injection of SkMb, MSC, and Fibro show retention not only in the heart, but also in the lungs (red arrows). Decreasing signal intensity over time is indicative of acute donor cell death in these groups. Scale bars represent BLI signal in photons/s/cm^2/sr. (b) Quantification of BLI signals on fixed regions of interest (ROI) over the heart reveal an early increase in signal from day 2 until day 7 in the MN group, while signal intensity in the SkMb (c), MSC (d), and Fibro (e) groups clearly decreases until background signal (black bars) at week 3 to 4. Bars represent mean ± SEM.

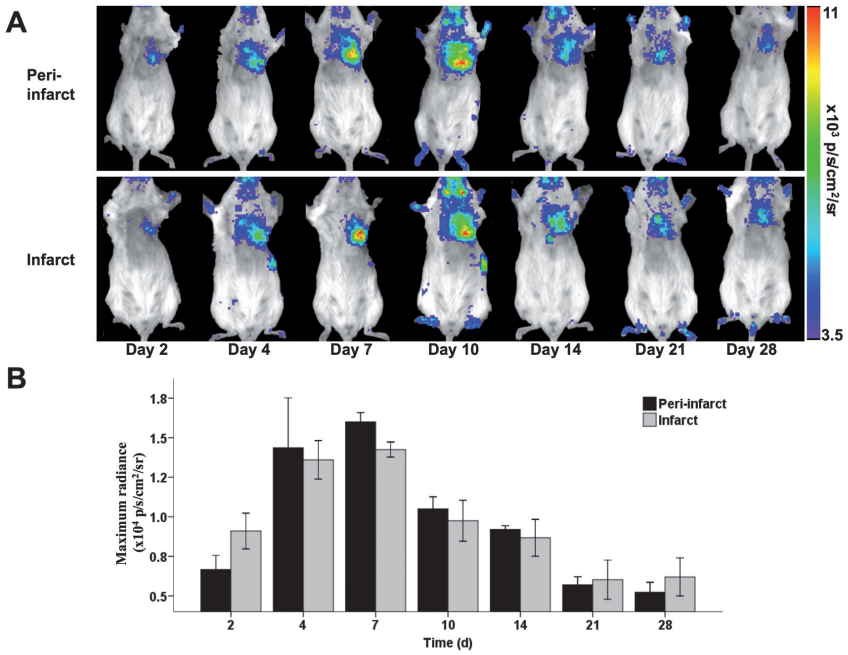

Figure 4. Cardiac injection site does not affect MN survival. (a) Pictures of representative animals injected with MN at the infarct versus peri-infarct zone. Note the acute proliferation phase from day 2 to day 7 followed by cell death from day 7 to day 28. Scale bars represent BLI signal in photons/s/cm^2/sr. (b) Graphic representation of quantified BLI signals on fixed regions of interest (ROI) over the heart showing similar cell survival patterns in both groups.

***Ex vivo* quantitative analysis of transplanted cells.** Previously, Muller-Ehmsen and colleagues have shown that post-mortem TaqMan PCR, which is based on the quantification of the Sry locus on the donor Y chromosome in the female recipient tissue, can be used to quantify cell survival in the heart.[17] To confirm increasing MN number during the first week, we explanted representative hearts on day 4 and 7, on which we performed *ex vivo* quantitative TaqMan PCR. Using a standard curve of cell number versus TaqMan cycle (data not shown), we were able to estimate the number of surviving cells. Indeed, this assay confirmed an increase in MN (2167±113 vs. 4408±544 cells, P<0.01) as shown in **figure 5a**. Next we performed TaqMan PCR on hearts injected with MN, SkMB, MSC, and Fibro at week 6 (n=6 per group). Similar to BLI data, the Taqman data confirmed the superior cell survival of MN (1853±568), which was significantly better than SkMb (97±62, *P*=0.001), MSC (341±192, *P*=0.005) and Fibro (no detectable cells, *P*<0.001, ANOVA) (**figure 5b**). Taken together, these *ex vivo* quantitative assays validate the *in vivo* BLI technique, suggesting that the latter can be used to follow cell fate in living subjects and may provide valuable insights into cell migration, proliferation, and death.

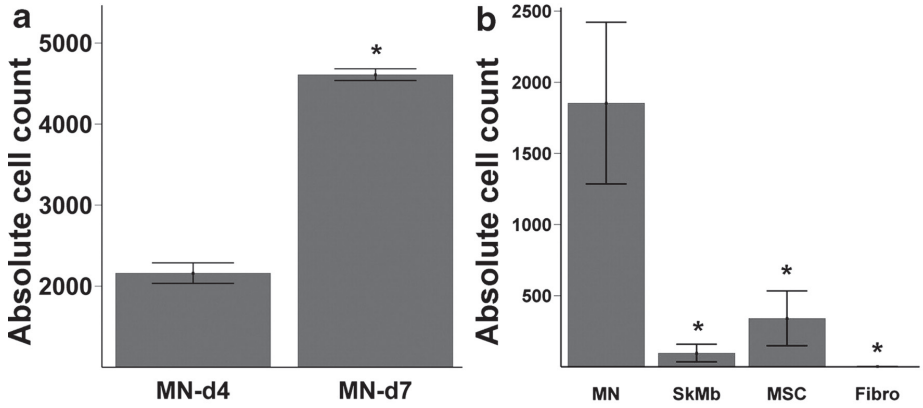

Figure 5. Ex vivo quantitative TaqMan PCR confirms BLI findings. (a) To confirm that the increase of MN signals actually represented increased MN in the hearts, ex vivo TaqMan PCR on extracted DNA from explanted hearts was conducted on day 4 and 7 (n=2 on both time points). TaqMan PCR cycle number was recalculated to absolute cell number using a simultaneously ran standard curve. Bars represent mean ± SEM. * represents P<0.05. (b) At week 6, significantly more MN cells were present in the recipient hearts compared to SkMB, MSC, and Fibro (n=6 per group). Bars represent mean ± SEM. * indicates MN vs. other groups: P<0.05.

Functional effects of cell transplantation. Echocardiographic measurements of cardiac performance were conducted 4 and 6 weeks after cell transplantation (**figure 6a**). At 6 weeks, LVFS for MN (37.1±2.5%) was significantly higher than PBS (30.2±1.9%, *P*<0.001) and Fibro (30.1±2.8%, *P*=0.004) groups. LVFS in the SkMb (35.2±1.8%) group was also significantly better than the PBS group (*P*=0.001), while MSC (32.4±2.1%) had no significant preservative effects compared to Fibro and PBS groups (repeated measurements ANOVA) (**figure 6b**). The LVFS in the PBS group was comparable with the literature.[18] Previously, it has been reported that cell transplantation accounted only for short-term preservation of cardiac function after MI.[19] In the present study, all cell groups showed decreased LVFS on week 6 compared to week 4. These findings suggest that the beneficial effects of cell transplantation may last only for the acute post MI period.

Validation of non-invasive measurements of left ventricular dimensions. Echocardiography readings from week 6 indicated that MN preserved both left-ventricular end-systolic (LVsd) and end-diastolic (LVdd) diameters (data not shown). To validate these findings, we performed invasive hemodynamic measurements. As expected, the left-ventricular end-systolic volume (Ves) 6 weeks after MN injection (42.6±2.0 µL) was significantly less than MSC (58.9±3.4 µL, *P*=0.002) and Fibro (65.1±2.7 µL, *P*<0.001), while the Ves after SkMb injection (49.7±2.7µL) was significantly decreased compared to Fibro (*P*=0.002). Moreover, the left-ventricular end-

diastolic volume (Ved) in the MN group (49.7±3.1 µL) was lower than all other groups and significantly decreased compared to Fibro (70.7±2.5 µL, $P<0.001$). No significant changes were observed in the SkMb (61.5±3.8 µL) and MSC (63.3±3.9 µL) groups (ANOVA). Importantly, these findings match the echocardiography results as mean values of LVsd vs. Ves and LVdd vs. Ved correlated robustly ($r^2=0.99$ and $r^2=0.88$, respectively, **figures 6c-d**).

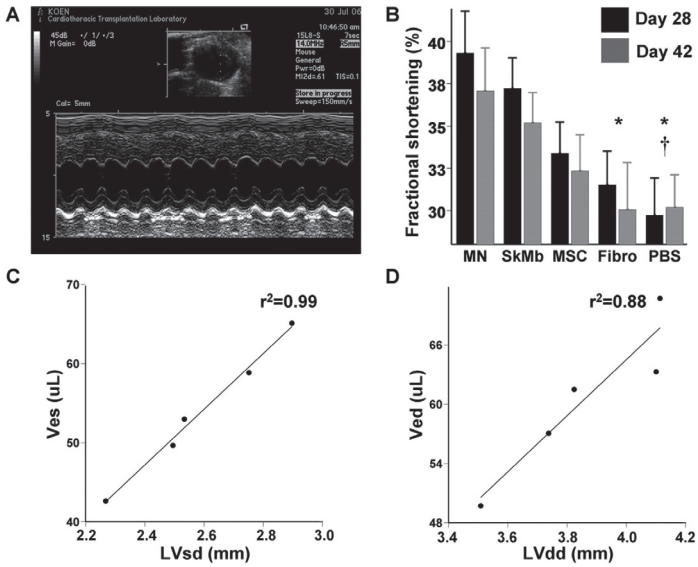

Figure 6. Measurements of functional consequences of cell transplantation into the infarcted mouse heart. (a) Representative M-mode traced picture taken at the level of the papillary muscle whereby left ventricular diameters can be measured. Scale bar is included on the left side. (b) Quantification of LVFS at 4 weeks (black) and 6 weeks (grey) after myocardial infarction and cell transplantation. MN appear to have the greatest functional protective effect compared to other groups. However, there is a general trend toward decreasing cardiac performance at 6 weeks instead. Immediately after echocardiography at week 6, invasive three-dimensional steady-state measurements of ventricular volumes at end-systole (Ves) and end-diastole (Ved) were conducted. Non-invasive echocardiography and invasive hemodynamic measurements correlate robustly between (c) Ves vs. LVsd ($r^2=0.99$) and (d) Ved vs. LVdd ($r^2=0.88$). Bars represent mean±SEM. MN (*) or SkMb (†) vs. indicated groups: $P<0.05$.

Transdifferentiation does not account for better cardiac performance. In our study, GFP-expressing MN could easily be found, confirming engraftment and BLI results (**figure 7**). However, histological samples showed no overlay of donor-specific GFP, nucleus-specific DAPI, and cardiac specific troponin I and connexin 43 markers two weeks after transplantation. Thus, concordant with earlier findings[15, 20], we have not observed MN-derived cardiomyocyte formation. Furthermore, we had difficulty identifying GFP-expressing SkMb, MSC, or Fibro, indicating that only very low counts of these cells were present in the heart (data not shown).

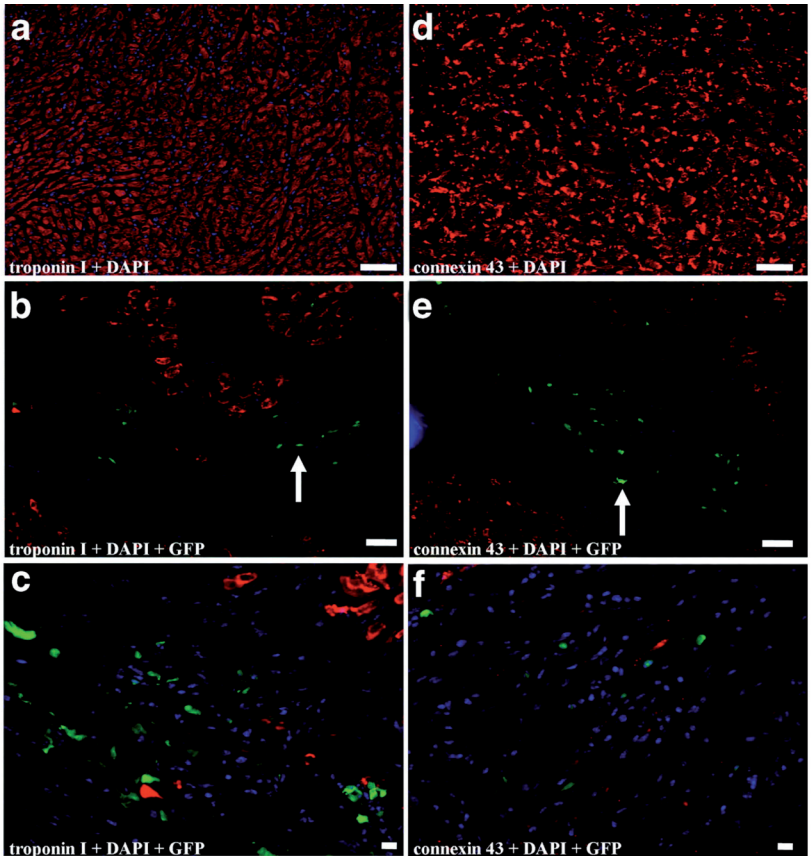

Figure 7. Immunohistochemical staining reveals no evidence of MN transdifferentiation into cardiomyocytes. (a) Representative figure with staining for (b-c) troponin I and DAPI. Although GFP-expressing MN can be found in the myocardium (arrow), there is no cell population with overlay of GFP, DAPI and troponin I to suggest transdifferentiation of MN to cardiomyocytes. (d) Representative figure with staining for (e-f) connexin 43 and DAPI. Although GFP-expressing MN can be found in the myocardium (arrow), there is no cell population with overlay of GFP, DAPI and connexin 43 to suggest transdifferentiation of MN to cardiomyocytes. Bars represent 50 μm.

DISCUSSION

This study is the first to evaluate the efficacy of three different clinical cell candidates for the treatment of myocardial infarction, as compared to a cellular control (Fibro) and non-cellular control (PBS). Our major findings are as follow: (1) molecular imaging using the Fluc reporter gene is a reliable tool for monitoring donor cell survival, proliferation and migration *in vivo*; (2) compared to SkMb, MSC and Fibro, MN show the most favorable survival pattern after injection into the infarcted heart; (3) MN injection leads to a better, but transient, preservation of cardiac function; and (4) this preservation is probably not due to substantial repopulation of the infarcted myocardium (as most cells die by imaging and TaqMan analysis) nor transdifferentiation into MN-derived cardiomyocytes.

Most animal studies assessing the therapeutic potential of cell therapy have used conventional, post-mortem histological or RT-PCR techniques to gain insight in donor cell location and count.[2] However, these techniques cannot monitor the kinetics of cell migration or cell survival in the same subject *in vivo*. In this respect, studies have shown the possibility of labeling donor cells with iron particles or radioactive probes to image cell location *in vivo*. Unfortunately, iron particles are non-specific, as they can be ingested by macrophages following transplanted cell death[21], and the relatively short half-lives of radioactive probes hamper long-term imaging of the cells.[9] By contrast, the current study demonstrates that molecular imaging of the Fluc reporter gene can provide longitudinal *in vivo* imaging of donor cell survival, proliferation, and migration and is in those aspects superior to the aforementioned imaging techniques. These advantages are a result of the stable genetic integration of the reporter gene (Fluc) in the donor cells, which are also equally transferred to progeny cells. As long as the donor/progeny cells are viable, transcription will lead to reporter gene mRNA followed by translation into reporter protein. Following systemic introduction, the reporter probe (D-Luciferin) will be catalyzed by all cells that have the reporter protein, leading to a signal which can be detected by a sensitive CCD camera.[22] However, due to the use of low-energy photons (2-3 eV), BLI is limited by photon attenuation and photon scattering within deep tissues. At present, this technique is not suitable for large animal or human studies.[23] Current studies in our laboratory are therefore aiming to combine multi-fusion reporter gene constructs (thereby enabling PET and BLI imaging) and iron labeling (for MRI).

Using *in vivo* BLI, *ex vivo* TaqMan PCR, and *ex vivo* histology, we have shown superior engraftment of MN compared to SkMB, MSC, and Fibro. Until now, little data exist on survival of transplanted cells in the infarcted heart. Müller-Ehmsen and colleagues used conventional PCR techniques to show that MN and MSC gradually died off until 6 weeks after transplantation of $1x10^5$ cells, with the percentage of engrafted MN being as low as ~2%. Moreover, the authors

found evidence of MN migration to spleen and liver.[24] Splenic and hepatic homing of MN, as also observed in this study, is most likely due to leakage from the initial injection. This has been shown earlier using RT-PCR in mice[24], SPECT imaging in large animal models[25], and PET imaging in humans.[26] In fact, the BLI findings of MN homing resemble leukocyte scans, showing white blood cells are effectively attracted by the liver and spleen.[27] The mechanism by which these organs retain circulating MN may be attributed to chemoattractant properties of the tissue or the biological role that these organs have. For example, the liver expresses high levels of stromal derived factor-1 (SDF-1), which is a developmental and postnatal chemoattractant for stem cells.[28] This has been extrapolated to cardiac stem cell therapy by exogenous myocardial SDF-1 over-expression, which improved the rate of c-kit$^+$ cell homing and improved LV function in hearts with post-infarction LV remodeling.[29]

In addition, increasing *in vivo* BLI signal during the first 2 weeks showed that MN were capable of either proliferation or homing in on the ischemic myocardium after an initial washout during this period of time, which was independent of injection site (infarct or peri-infarct). Although the survival pattern of MN was superior compared to other cell types, it must be stated that the cell number by TaqMan PCR at week 6 equaled ~1,800 cells, representing only ~0.4% of the initially injected cell number. For MSC, we found the *in vivo* imaging signals to decrease dramatically within one week. This pattern concurs with the findings from others who found drastic MSC death between day 3 and 7 after myocardial delivery.[30]

To date, there is intense investigative effort to uncover the mechanism by which stem cells may preserve the function of damaged hearts. Based on our current findings, the preservation of cardiac function by MN transplantation is not attributable to repopulation or transdifferentiation. Rather, the functional benefits of MN transplantation might be due to an augmentation of the natural process of myocardial healing by paracrine signaling and promoting neovascularization, among other factors. It has recently been shown that mice over-expressing MCP-1, which leads to an increased influx of MN into the damaged myocardium after infarction, had decreased infarcted areas and scar formation, and yielded better left ventricular function compared to wild-type mice.[31] Moreover, in the infarcted myocardium, CD11b$^+$ macrophages are an important source of cytokines and growth factors[32] and potential regulators of the extracellular matrix synthesis.[33] Specifically, transplantation of activated macrophages into the infarcted rat heart has been shown to accelerate vascularization and tissue repair and to improve cardiac remodeling and function.[34] Regarding paracrine signaling, bone marrow stem cells can secrete vascular endothelial growth factor (VEGF), basic fibroblast growth factor (bFGF), angiopoetin-1 (Ang-1), and monocyte chemoattractant protein-1 (MCP-1), leading to an increase in collateral perfusion and cardiac function in pigs with myocardial infarction.[35, 36] Concordantly,

results from the Doppler substudy of the REPAIR-AMI trial have recently shown clinical proof of restored microvascular function associated with an improved maximal vascular conductance capacity.[37]

The clinical relevance of this study is significant. Different clinical trials have been conducted with divergent results that raise questions about which optimal cell type to use.[8] Although each cell type has its own advantages and limitations, our study is the first to detect a clear survival and modest functional benefit of MN compared to other clinical cellular candidates. However, questions remain regarding which portion of MN is responsible for the benefit, whether this benefit is transient, and whether a significant difference in cardiac function could translate into a clinical difference. These issues need to be addressed in future studies. Nevertheless, by using multi-modality evaluation, this study has demonstrated that MN confer a survival pattern in the infarcted mouse heart superior to those of SkMb and MSC. Moreover, MN exhibited a modest but transient preservation of cardiac function compared to cellular and non-cellular controls. Finally, our findings highlight the importance of being able to track stem cells *in vivo* and should be an impetus for further research on the development of clinically applicable molecular imaging techniques to closely follow stem cell fate in humans.

ACKNOWLEDGEMENTS

The authors thank V. Mariano for animal care, P. Chu for assistance with histology, and R. Wolterbeek for statistical advice. This work was supported in part by grants from the NIH HL089027, NIH HL074883, and Burroughs Wellcome Foundation Career Award for Medical Scientist (JCW). K.E.A. van der Bogt was supported by the American Heart Association (Medical Student Research Award), Fulbright committee, VSB fund, Michael van Vloten fund, and Jo Keur Grant.

REFERENCES

1. Rosamond W, Flegal K, Friday G, Furie K, Go A, Greenlund K, Haase N, Ho M, Howard V, Kissela B, Kittner S, Lloyd-Jones D, McDermott M, Meigs J, Moy C, Nichol G, O'Donnell C J, Roger V, Rumsfeld J, Sorlie P, Steinberger J, Thom T, Wasserthiel-Smoller S, Hong Y. Heart Disease and Stroke Statistics--2007 Update. A Report From the American Heart Association Statistics Committee and Stroke Statistics Subcommittee. *Circulation.* 2006.
2. Laflamme MA, Murry CE. Regenerating the heart. *Nat Biotechnol.* 2005;23(7):845-856.
3. Hagege AA, Marolleau JP, Vilquin JT, Alheritiere A, Peyrard S, Duboc D, Abergel E, Messas E, Mousseaux E, Schwartz K, Desnos M, Menasche P. Skeletal myoblast transplantation in ischemic heart failure: long-term follow-up of the first phase I cohort of patients. *Circulation.* 2006;114(1 Suppl):I108-113.
4. Lunde K, Solheim S, Aakhus S, Arnesen H, Abdelnoor M, Egeland T, Endresen K, Ilebekk A, Mangschau A, Fjeld JG, Smith HJ, Taraldsrud E, Grogaard HK, Bjornerheim R, Brekke M, Muller C, Hopp E, Ragnarsson A, Brinchmann JE, Forfang K. Intracoronary injection of mononuclear bone marrow cells in acute myocardial infarction. *N Engl J Med.* 2006;355(12):1199-1209.
5. Assmus B, Honold J, Schachinger V, Britten MB, Fischer-Rasokat U, Lehmann R, Teupe C, Pistorius K, Martin H, Abolmaali ND, Tonn T, Dimmeler S, Zeiher AM. Transcoronary transplantation of progenitor cells after myocardial infarction. *N Engl J Med.* 2006;355(12):1222-1232.
6. Schachinger V, Erbs S, Elsasser A, Haberbosch W, Hambrecht R, Holschermann H, Yu J, Corti R, Mathey DG, Hamm CW, Suselbeck T, Assmus B, Tonn T, Dimmeler S, Zeiher AM. Intracoronary bone marrow-derived progenitor cells in acute myocardial infarction. *N Engl J Med.* 2006;355(12):1210-1221.
7. Chen SL, Fang WW, Ye F, Liu YH, Qian J, Shan SJ, Zhang JJ, Chunhua RZ, Liao LM, Lin S, Sun JP. Effect on left ventricular function of intracoronary transplantation of autologous bone marrow mesenchymal stem cell in patients with acute myocardial infarction. *Am J Cardiol.* 2004;94(1):92-95.
8. Rosenzweig A. Cardiac cell therapy--mixed results from mixed cells. *N Engl J Med.* 2006;355(12):1274-1277.
9. Chang GY, Xie X, Wu JC. Overview of stem cells and imaging modalities for cardiovascular diseases. *J Nucl Cardiol.* 2006;13(4):554-569.
10. Cao F, Van Der Bogt KE, Sadrzadeh A, Xie X, Sheikh AY, Wang H, Connolly AJ, Robbins RC, Wu JC. Spatial and temporal kinetics of teratoma formation from murine embryonic stem cell transplantation. *Stem Cells Dev.* 2007.
11. Cao YA, Wagers AJ, Beilhack A, Dusich J, Bachmann MH, Negrin RS, Weissman IL, Contag CH. Shifting foci of hematopoiesis during reconstitution from single stem cells. *Proc Natl*

Acad Sci U S A. 2004;101(1):221-226.

12. Salmon AB, Murakami S, Bartke A, Kopchick J, Yasumura K, Miller RA. Fibroblast cell lines from young adult mice of long-lived mutant strains are resistant to multiple forms of stress. *Am J Physiol Endocrinol Metab.* 2005;289(1):E23-29.
13. Rando TA, Blau HM. Primary mouse myoblast purification, characterization, and transplantation for cell-mediated gene therapy. *J Cell Biol.* 1994;125(6):1275-1287.
14. Cao F, Lin S, Xie X, Ray P, Patel M, Zhang X, Drukker M, Dylla SJ, Connolly AJ, Chen X, Weissman IL, Gambhir SS, Wu JC. In vivo visualization of embryonic stem cell survival, proliferation, and migration after cardiac delivery. *Circulation.* 2006;113(7):1005-1014.
15. Balsam LB, Wagers AJ, Christensen JL, Kofidis T, Weissman IL, Robbins RC. Haematopoietic stem cells adopt mature haematopoietic fates in ischaemic myocardium. *Nature.* 2004;428(6983):668-673.
16. Dziennis S, Van Etten RA, Pahl HL, Morris DL, Rothstein TL, Blosch CM, Perlmutter RM, Tenen DG. The CD11b promoter directs high-level expression of reporter genes in macrophages in transgenic mice. *Blood.* 1995;85(2):319-329.
17. Muller-Ehmsen J, Whittaker P, Kloner RA, Dow JS, Sakoda T, Long TI, Laird PW, Kedes L. Survival and development of neonatal rat cardiomyocytes transplanted into adult myocardium. *J Mol Cell Cardiol.* 2002;34(2):107-116.
18. Rohde LE, Ducharme A, Arroyo LH, Aikawa M, Sukhova GH, Lopez-Anaya A, McClure KF, Mitchell PG, Libby P, Lee RT. Matrix metalloproteinase inhibition attenuates early left ventricular enlargement after experimental myocardial infarction in mice. *Circulation.* 1999;99(23):3063-3070.
19. Dai W, Hale SL, Martin BJ, Kuang JQ, Dow JS, Wold LE, Kloner RA. Allogeneic mesenchymal stem cell transplantation in postinfarcted rat myocardium: short- and long-term effects. *Circulation.* 2005;112(2):214-223.
20. Murry CE, Soonpaa MH, Reinecke H, Nakajima H, Nakajima HO, Rubart M, Pasumarthi KB, Virag JI, Bartelmez SH, Poppa V, Bradford G, Dowell JD, Williams DA, Field LJ. Haematopoietic stem cells do not transdifferentiate into cardiac myocytes in myocardial infarcts. *Nature.* 2004;428(6983):664-668.
21. Terrovitis J, Stuber M, Youssef A, Preece S, Leppo M, Kizana E, Schar M, Gerstenblith G, Weiss RG, Marban E, Abraham MR. Magnetic Resonance Imaging Overestimates Ferumoxide-Labeled Stem Cell Survival After Transplantation in the Heart. *Circulation.* 2008.
22. van der Bogt KE, Swijnenburg RJ, Cao F, Wu JC. Molecular imaging of human embryonic stem cells: keeping an eye on differentiation, tumorigenicity and immunogenicity. *Cell Cycle.* 2006;5(23):2748-2752.
23. Li Z, Suzuki Y, Huang M, Cao F, Xie X, Connolly AJ, Yang PC, Wu JC. Comparison of Reporter Gene and Iron Particle Labeling for Tracking Fate of Human Embryonic Stem

Cells and Differentiated Endothelial Cells in Living Subjects. Stem Cells. 2008.

24. Muller-Ehmsen J, Krausgrill B, Burst V, Schenk K, Neisen UC, Fries JW, Fleischmann BK, Hescheler J, Schwinger RH. Effective engraftment but poor mid-term persistence of mononuclear and mesenchymal bone marrow cells in acute and chronic rat myocardial infarction. *J Mol Cell Cardiol.* 2006;41(5):876-884.
25. Hou D, Youssef EA, Brinton TJ, Zhang P, Rogers P, Price ET, Yeung AC, Johnstone BH, Yock PG, March KL. Radiolabeled cell distribution after intramyocardial, intracoronary, and interstitial retrograde coronary venous delivery: implications for current clinical trials. *Circulation.* 2005;112(9 Suppl):I150-156.
26. Hofmann M, Wollert KC, Meyer GP, Menke A, Arseniev L, Hertenstein B, Ganser A, Knapp WH, Drexler H. Monitoring of bone marrow cell homing into the infarcted human myocardium. *Circulation.* 2005;111(17):2198-2202.
27. Datz FL, Luers P, Baker WJ, Christian PE. Improved detection of upper abdominal abscesses by combination of 99mTc sulfur colloid and 111In leukocyte scanning. *AJR Am J Roentgenol.* 1985;144(2):319-323.
28. Kucia M, Reca R, Miekus K, Wanzeck J, Wojakowski W, Janowska-Wieczorek A, Ratajczak J, Ratajczak MZ. Trafficking of normal stem cells and metastasis of cancer stem cells involve similar mechanisms: pivotal role of the SDF-1-CXCR4 axis. *Stem Cells.* 2005;23(7):879-894.
29. Zhang G, Nakamura Y, Wang X, Hu Q, Suggs LJ, Zhang J. Controlled release of stromal cell-derived factor-1 alpha in situ increases c-kit+ cell homing to the infarcted heart. *Tissue Eng.* 2007;13(8):2063-2071.
30. Mangi AA, Noiseux N, Kong D, He H, Rezvani M, Ingwall JS, Dzau VJ. Mesenchymal stem cells modified with Akt prevent remodeling and restore performance of infarcted hearts. *Nat Med.* 2003;9(9):1195-1201.
31. Morimoto H, Takahashi M, Izawa A, Ise H, Hongo M, Kolattukudy PE, Ikeda U. Cardiac overexpression of monocyte chemoattractant protein-1 in transgenic mice prevents cardiac dysfunction and remodeling after myocardial infarction. *Circ Res.* 2006;99(8):891-899.
32. Frangogiannis NG, Smith CW, Entman ML. The inflammatory response in myocardial infarction. *Cardiovasc Res.* 2002;53(1):31-47.
33. Frangogiannis NG, Mendoza LH, Lindsey ML, Ballantyne CM, Michael LH, Smith CW, Entman ML. IL-10 is induced in the reperfused myocardium and may modulate the reaction to injury. *J Immunol.* 2000;165(5):2798-2808.
34. Leor J, Rozen L, Zuloff-Shani A, Feinberg MS, Amsalem Y, Barbash IM, Kachel E, Holbova R, Mardor Y, Daniels D, Ocherashvilli A, Orenstein A, Danon D. Ex vivo activated human macrophages improve healing, remodeling, and function of the infarcted heart. *Circulation.* 2006;114(1 Suppl):I94-100.

35. Fuchs S, Baffour R, Zhou YF, Shou M, Pierre A, Tio FO, Weissman NJ, Leon MB, Epstein SE, Kornowski R. Transendocardial delivery of autologous bone marrow enhances collateral perfusion and regional function in pigs with chronic experimental myocardial ischemia. *J Am Coll Cardiol.* 2001;37(6):1726-1732.
36. Kamihata H, Matsubara H, Nishiue T, Fujiyama S, Tsutsumi Y, Ozono R, Masaki H, Mori Y, Iba O, Tateishi E, Kosaki A, Shintani S, Murohara T, Imaizumi T, Iwasaka T. Implantation of bone marrow mononuclear cells into ischemic myocardium enhances collateral perfusion and regional function via side supply of angioblasts, angiogenic ligands, and cytokines. *Circulation.* 2001;104(9):1046-1052.
37. Erbs S, Linke A, Schachinger V, Assmus B, Thiele H, Diederich KW, Hoffmann C, Dimmeler S, Tonn T, Hambrecht R, Zeiher AM, Schuler G. Restoration of microvascular function in the infarct-related artery by intracoronary transplantation of bone marrow progenitor cells in patients with acute myocardial infarction: the Doppler Substudy of the Reinfusion of Enriched Progenitor Cells and Infarct Remodeling in Acute Myocardial Infarction (REPAIR-AMI) trial. *Circulation.* 2007;116(4):366-374.